



Least-squares based coulomb counting method and its application for state-of-charge (SOC) estimation in electric vehicles

Li Zhao^{1,2}, Muyi Lin^{1,3} and Yong Chen^{1,3,*†}

¹Collaborative Innovation Center of Electric Vehicles in Beijing, Beijing Information Science and Technology University, Beijing 100192, China

²National Engineering Laboratory for Electric Vehicles, Beijing Institute of Technology, Beijing 100081, China

³State Key Laboratory of Automotive Safety and Energy, Beijing 100084, China

SUMMARY

Coulomb counting method is a convenient and straightforward approach for estimating the state-of-charge (SOC) of lithium-ion batteries. Without interrupting the power supply, the remaining capacities of them in an electric vehicle (EV) can be calculated by integrating the current leaving and entering the batteries. The main drawbacks of this method are the cumulative errors and the time-varying coulombic efficiency, which always lead to inaccurate estimations. To deal with this problem, a least-squares based coulomb counting method is proposed. With the proposed method, the coulombic losses can be compensated by charging/discharging coulombic efficiency η and the measurement drift can be amended with a morbid efficiency matrix. The experimental results demonstrated that the proposed method is effective and convenient.

Copyright © 2016 John Wiley & Sons, Ltd.

KEY WORDS

coulomb counting method; state of charge (SOC); coulombic efficiency (CE); least squares (LS)

Correspondence

*Yong Chen, Mechanical Electrical Engineering School, Beijing Information Science and Technology University, Beijing 100192, China.

†E-mail: chen_yong_jz@126.com

Accepted 27 February 2015; Received 13 July 2015; Revised 25 February 2015

1. INTRODUCTION

State-of-charge (SOC) and residual capacity (RC) estimation is important issues for battery management system in electric vehicles (EVs) [1–3]. Because there is no historical information about the charging and discharging progress, it is very difficult to accurately estimate SOC or RC from real-time measurement information. It is very hard to avoid unpredicted-system-interruptions [4,5]. Although many electrochemical methods have been proposed and the accuracies of them have been verified, estimating the SOC or RC for commercial batteries in EVs is still a quite challenging work for no destructive measurement and power supply interruption is permitted.

Up to now, many SOC or RC estimation methods have been proposed, and most of them estimate the battery state with indirect parameters, which change irregularly with the charging/discharging rate, depth-of-discharge (DOD) and ambient temperatures [6–8]. Thus, the SOC estimation methods, relying on these indirect parameters, can hardly

obtain precise estimation results. The discharge test method is a reliable method to determine the SOC of batteries, and the remained charge can be precisely calculated with it [9–11]. However, the consumed time is very long, and after test, no power is left in the battery. Open circuit voltage (OCV) method is another frequently-used method for SOC calibration, and there is a one-to-one correspondence between SOC and OCV [12,13]. Whereas, the lengthy time for state-switching appeared in the charge/discharge process makes it unusable for EVs in driving status. The model based method dynamically estimates SOC with precise and complex battery models [14–16], the expensive computation cost of which makes itself unsuitable for EVs with limited calculation resources. The neural network method can deal with different kinds of batteries, but the great number of training samples and training procedures needed by this method prevents its further application [17,18].

On the contrary, the coulomb counting method calculates SOC or RC by accumulating the value of the direct

parameter—current [19,20]. This is a simple and general method, and the precision of it is decided mainly by the sampling precision and frequency of the current sensor. Nowadays, various portable devices and EVs, consisting of computable hardware and large size of memory, estimate the remaining capacities with this method [21]. As an open loop SOC estimating method, the errors of the coulomb counting method are accumulated in the current measuring process. With the increasing of the detecting time, the cumulative error becomes more and more large [22,23]. In fact, the estimation result of it is largely influenced by the precision of the current sensor, especially by the measurement drift, which will result in cumulative effects [24,25]. Additionally, the method does not take into account the age and capacity changes of the battery. For a battery, the CE of it is greatly influenced by the operating state of battery (SOC, temperature, current, etc), and it is difficult to be measured [26–29]. For lithium-ion battery, its cycle life is not infinite, and many factors give their effects on capacity fade and electrolyte oxidation, although the CE of it is relatively high and stable than other batteries. Thus, disadvantages of this method hinder its further application [30].

To deal with this problem, we proposed a least squares based coulomb counting method for estimating the RC or SOC of lithium-ion batteries. The initial SOC of the tested battery is obtained from the OCV. The charging/discharging efficiencies, used for compensating the coulombic losses, are periodically calibrated by the method of least squares. The measurement drift, coming from current sensor, is amended with the accumulated capacity and the modified efficiency matrix. The rest of this paper is organized as follows. We first review the basic coulomb counting method and the definition of coulombic efficiency. Second, we represent the LS-based coulomb counting method for lithium-ion batteries. Then we describe several experiments, in which we demonstrated how to accumulate the summary information and to calculate the SOC or RC with the proposed algorithm. Finally, we conclude this paper by highlighting the key contributions of this work.

2. THE LS-BASED SOC OR RC ESTIMATING METHOD

2.1. Coulomb counting method

Coulomb counting method (Ampere-Hour integral method) is the most common and straightforward method for estimating battery SOC. Many battery management systems calculate SOC with the basic coulomb counting method or its variations [19,20,23]. In these approaches, the current leaving and entering the battery is calculated periodically, and the SOC of the battery is estimated by subtracting or adding the cumulative net charge.

Definition 1. (State of charge, SOC). Let C_N be the rated capacity of a battery, $SOC(t_0)$ be the SOC at the initial time t_0 , η be the coulombic efficiency, $I(t)$ be the current which is positive at discharge and negative at charge, with the measured current, the SOC obtained with Ampere-Hour integral method could be represented by

$$SOC(t) = SOC(t_0) - \frac{1}{C_N} \int_{t_0}^t \eta \cdot I(t) \cdot dt \quad (1)$$

Usually, the initial SOC, $SOC(t_0)$, can be estimated by the open-circuit voltage based approach or the extended Kalman filter based approach [12,13]. The rated capacity, C_N , can be obtained from battery manufacturer or be measured in laboratory. The precise current, $I(t)$, can be obtained by investing more money in the measuring equipment. However, accurate coulombic efficiency, η , cannot be simply estimated with common methods. In fact, the value of η keeps on changing in the whole discharging or charging process. Replacing the real value of η with an average value or an estimated one is not a feasible way for SOC estimating. The charge or discharge current, temperature, SOC range, state of health (SOH), the characteristics of the battery itself and many other factors impose their influences on the coulombic efficiency in the calculating process. In fact, SOH is a metric which indicates the battery condition related to a new battery. In the proposed algorithm, SOH is defined as the ratio of the available capacity and its rated capacity.

2.2. Coulombic efficiency (η)

Definition 2. (Coulombic efficiency, η). Let I_d be the discharge current, I_c be the charge current, t_d be the discharge time and t_c be the charge time, the coulombic efficiency of the tested battery, η , could be represented by

$$\eta = \int_0^{t_d} I_d dt / \int_0^{t_c} I_c dt \quad (2)$$

Definition 3. (Charge coulombic efficiency, $\eta_{c,In}$). Discharge a battery at C/3 rate until the terminal voltage is reached, and then, charge it at a certain current I_n until SOC=1. The charged capacity is $Q_{c,In} = I_n \cdot t_{c,In}$, where $t_{c,In}$ is the charge time. Have a rest for 10 min and then discharge the battery at C/3 rate until his terminal voltage. The discharged capacity is $Q_{d,C/3} = (C/3) \cdot t_{d,C/3}$, where $t_{d,C/3}$ is the discharge time. Thus, the charge coulombic efficiency can be calculated like this,

$$\eta_{c,I_n} = Q_{d,C/3} / Q_{c,I_n} = \left(\frac{C}{3} t_{d,C/3} \right) / (I_n \cdot t_{c,I_n}) \quad (3)$$

Definition 4. (Discharge coulombic efficiency, $\eta_{d,In}$). Discharge a battery with current I_n until the terminal voltage is reached, and then, charge it at C/3 rate until SOC=1. The

charged capacity is $Q_{c,C/3} = (C/3) \cdot t_{c,C/3}$, where $t_{c,C/3}$ is the charge time. Have a rest for 10 min and then discharge the battery at a current I_n until his terminal voltage. The discharged capacity is $Q_{d,I_n} = (I_n) t_{d,I_n}$, where t_{d,I_n} is the discharge time. Thus, the discharge coulombic efficiency can be calculated like this,

$$\eta_{d,I_n} = Q_{d,I_n} / Q_{c,C/3} = (I_n \cdot t_{d,I_n}) / \left(\frac{C}{3} t_{c,C/3} \right) \quad (4)$$

In fact, in the charge/discharge process, the energy loss of the battery is inevitable. In the laboratory conditions, the average coulombic efficiency, η , can be calculated by formula (2). However, in the actual conditions, the charge and discharge process in EV keeps alternating and all of the factors, current, temperature and capacity, change continuously and sharply. It is hard to find an effective method or equipment to calculate the average coulombic efficiency accurately. For example, the charge and discharge coulombic efficiencies of a given cell are shown in Figure 1(a) and (b). The coulombic efficiencies on different temperatures and SOC are shown in (c) and (d). The calculating method of them can be seen in [19]. From Figure 1(a)–(d), we can see that the changing range of the coulombic efficiency of the battery is very large. **Without recording all of the detail charge/discharge information, it is impossible to obtain an accurate SOC estimation.**

2.3. LS-based SOC or RC estimating method

In fact, in actual driving conditions, it is very hard to accurately calculate SOC or RC with an estimated coulombic efficiency needed by formula (1) in the whole charge or

discharge process. So many factors give their effects on coulombic efficiency and calculating result. **Thus, accumulating the measured current and correcting it with accurate coulombic efficiency at each measurement point perhaps is the only feasible way.** In such a condition, formula (1) can be replaced by (5) where $I(t)$, $T(t)$, $SOC(t)$ and $SOH(t)$ are the current, temperature, SOC and SOH of the battery at time t .

$$SOC(t) = SOC(t_0) - \frac{1}{C_N} \int_{t_0}^t \eta[I(t), T(t), SOC(t), SOH(t)] \cdot I(t) \cdot dt \quad (5)$$

In practice, sensors can only send data at every discrete time point, t_k ($t_k = \Delta t \times k$). Δt is the sampling interval and k is the number of sampling. Thus, we can get,

$$SOC(t) \approx SOC(t_0) - \frac{1}{C_N} \cdot \sum_{k=\Delta t \times 0}^{\Delta t \times k} \eta[I(t_k), T(t_k), SOC(t_k), SOH(t_k)] \cdot I(t_k) \cdot \Delta t \quad (6)$$

Generally speaking, the definition domain of coulombic efficiency, η , is continuous. It is impossible to obtain such an accurate value for each independent variable in its definition domain. Thus, we have to discretize its definition domain into lattices with the same size. **In the same lattice, the coulombic efficiencies of these points are set to the same.** Thus,

$$SOC(t) \approx SOC(t_0) - \frac{1}{C_N} \cdot \sum_{k=\Delta t \times 0}^{\Delta t \times k} \eta [I^*(t_k), T^*(t_k), SOC^*(t_k), SOH^*(t_k)] \cdot I(t_k) \cdot \Delta t$$

where $I^*(t_k)$, $T^*(t_k)$, $SOC^*(t_k)$ and $SOH^*(t_k)$ are the discretized values for $I(t_k)$, $T(t_k)$, $SOC(t_k)$ and $SOH(t_k)$.

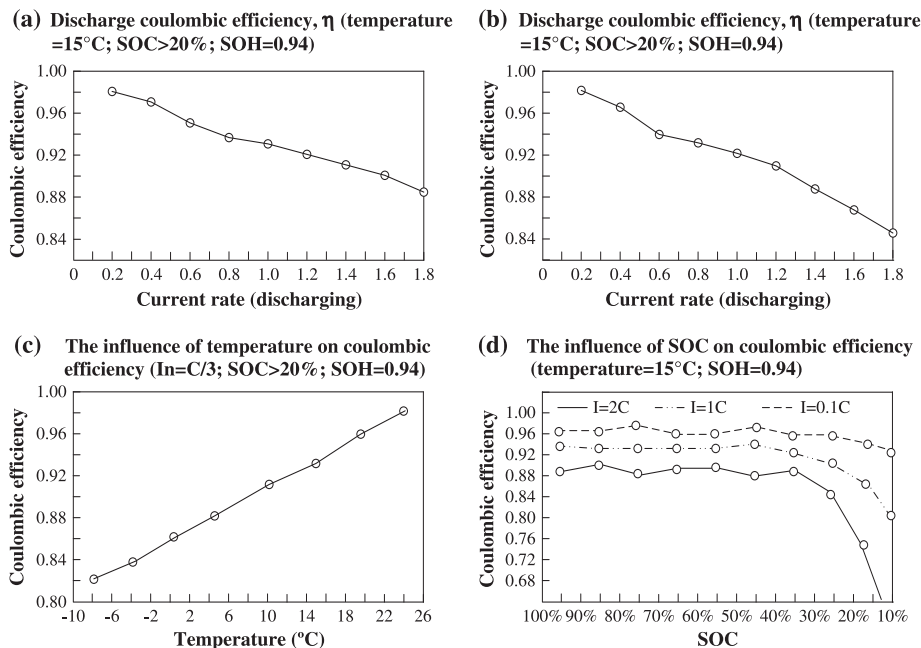


Figure 1. The influences of discharge/charge current, temperature and available capacity on coulombic efficiency.

Having discretized the whole definition domain into lattices and calculated the whole capacity for each lattice, we can number these lattices with 'L1, L2, ..., Ln' and calculate the SOC of battery with formula (5),

$$SOC(t) \approx SOC(t_0) - \frac{1}{C_N} \cdot [\eta_{L1} \cdot Q_{L1} + \eta_{L2} \cdot Q_{L2} + \dots + \eta_{Ln} \cdot Q_{Ln}] \quad (7)$$

In (7), L_i is a discretized combination of I^* , T^* , SOC^* and SOH^* . Q_{L_i} is the total charge taken out of the battery when the battery is in state L_i .

In fact, accurately determining these coulombic efficiencies, η_{L_i} , is a hard thing. The relationship between the discharge capacity and the operating current/battery temperature/SOH is complicated and nonlinear. The discharged/charged capacity of a battery can be expressed like this,

$$Q^* \approx C_N \times [SOC(t_0) - SOC(t)] \approx \eta_{L1} \cdot Q_{L1} + \eta_{L2} \cdot Q_{L2} + \dots + \eta_{Ln} \cdot Q_{Ln} \quad (8)$$

For an EV, after the k^{th} driving cycle, the discharged/charged capacity Q_k^* can be expressed like this,

$$Q_k^* = \eta \times Q_k + \epsilon_k$$

where $\eta = \{\eta_{L1}, \eta_{L2}, \dots, \eta_{Ln}\}$ be the vector of coulombic efficiency, $Q_k = \{Q_{L1,k}, Q_{L2,k}, \dots, Q_{Ln,k}\}$ be the accumulated capacities for lattices and ϵ_k be the error.

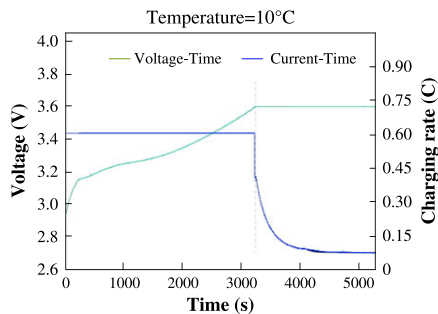
After K cycles, we obtained the matrix,

$$\begin{cases} Q_1^* = \eta_{L1} \cdot Q_{L1,1} + \eta_{L2} \cdot Q_{L2,1} + \dots + \eta_{Ln} \cdot Q_{Ln,1} + \epsilon_1 \\ Q_2^* = \eta_{L1} \cdot Q_{L1,2} + \eta_{L2} \cdot Q_{L2,2} + \dots + \eta_{Ln} \cdot Q_{Ln,2} + \epsilon_2 \\ \dots \\ Q_K^* = \eta_{L1} \cdot Q_{L1,K} + \eta_{L2} \cdot Q_{L2,K} + \dots + \eta_{Ln} \cdot Q_{Ln,K} + \epsilon_K \end{cases}$$

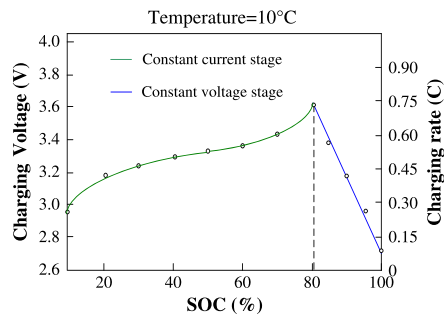
There are many methods can be used for estimating the unknown parameter η as long as $Ln \leq K$. In this paper, we estimate η with least square method. The sum of squares to be minimized is

$$S = \sum_{k=1}^K (Q_k^* - \eta Q_k)^2 \quad (9)$$

Thus, the least squares estimate of coulombic efficiency, η^* , is given by



(a) Charging current and voltage



(b) The relationship between SOC and voltage/current

Figure 2. The charging voltage, current and SOC estimation curves.

$$\eta^* = \frac{\sum_k Q_k Q_k^*}{\sum_k Q_k^2} \quad (10)$$

In this way, coulombic efficiency, η , can be calculated after K time running and can be updated every time a charge-discharge cycle has been completed.

3. DETERMINATION OF INITIAL SOC

For an EV, the initial SOC can be easily obtained after two stages, charging stage and open-circuit stage. There exists a special relationship curve between SOC and other parameters in the two stages when a standard condition is given. However, in running stage, the situation is very complex. An accurate SOC cannot be obtained by simply accumulating the discharge current. It needs continuous revisions for eliminating the errors coming from measurement drift and coulombic loss. Thus, in the proposed algorithm, the charging and open-circuit stages are used to calculate the initial SOC, and the running stage is used to revise the values of coulombic efficiencies. Every time a long time rest or a standard charging stage takes place, the initial SOC will be re-calibrated. After each discharging stage, the accumulated capacities for different lattices will be used to build a new equation for calibrating the coulombic efficiency, η .

3.1. Charging stage

$$I = \frac{58.75mA}{2350Ah} = 0.025C$$

Figure 2(a) indicates the variation of the battery voltage and current when the tested battery is charged. In this experiment, the battery is first charged with a constant rate of 0.6C to a threshold voltage of 3.6 V, and then charged with a constant voltage of 3.6 V to its full capacity. It can be observed that with the constant charging current, the battery voltage increases gradually and reaches the threshold after 3200 s. After that, the battery charged by the constant-voltage mode and the charging current drops rapidly in the first step, and then slowly. When the current declines to 0.1C, the charging stage closes. The relationship between SOC and charging voltage during the constant-current stage or the relationship between SOC

and charging current during the constant-voltage stage can be seen in Figure 2(b). With the two charging curves, we can calculate the initial SOC in every charging time.

3.2. Open circuit stage

For the tested battery, after 60-min rest, the relationship between the SOC and the open-circuit-voltage is shown in Figure 3. Although the battery can be discharged at different rates before disconnecting from load, after a long period rest time, the curves (open-circuit-voltage VS SOC) of them are very similar. Thus, we can repeatedly calibrate the initial SOC and revise the coulombic efficiency, η , after every open circuit stage.

4. ESTIMATING SOC OR RC FOR BATTERIES

4.1. Reducing the dimension of coulombic efficiency, η

From formulas (5)–(8) we can find that the coulombic efficiency η is a function of discharge/charge current, temperature, SOC and SOH. If we discretize the definition domains into lattices for each of the four dimensions, the number of lattices will be very large, and the calculation cost will be very expensive. In fact, SOH is a slow-changing parameter for batteries in EVs. For a short-term of running (several driving cycles), we can assume that SOH gives no influence on coulombic efficiency.

Additionally, from Figure 1(d) we can find that if the SOC keeps in the area of 100%–25% in the charge/discharge process, the coulombic efficiency η keeps unchanged approximately. Thus, by setting an appropriate discharge voltage threshold, we can ignore the impact of SOC. After doing so, we can reduce the dimensions of coulombic efficiencies and discretize them formally. The results are shown in Table I.

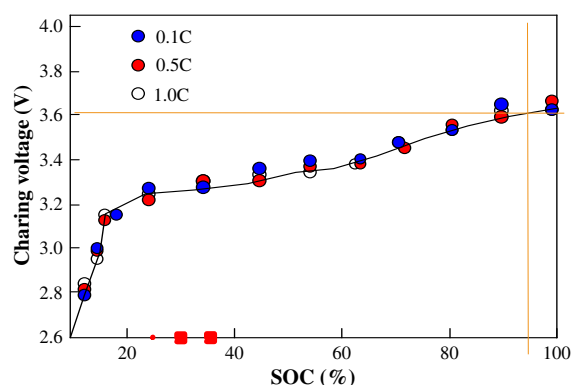


Figure 3. The estimation curves in open-circuit stage.

Table I. The discretized coulombic efficiency.

Coulombic efficiency (η)		Temperature ($^{\circ}\text{C}$)						
		-10	-5	0	5	10	15	20
Current	0.2C	0.95	0.96	0.97	0.98	0.98	0.99	0.99
	0.4C	0.94	0.95	0.96	0.97	0.97	0.98	0.99
	0.6C	0.93	0.94	0.96	0.96	0.96	0.97	0.98
	0.8C	0.91	0.93	0.94	0.95	0.95	0.96	0.97
	1.0C	0.90	0.92	0.93	0.94	0.94	0.95	0.96
	1.2C	0.89	0.91	0.92	0.93	0.93	0.94	0.95
	1.4C	0.88	0.89	0.90	0.91	0.92	0.93	0.94

4.2. Calculating the accumulated capacities for lattices

Generally speaking, in a driving cycle (EV), the accumulated capacities of lattices are very different. This can be observed in Figure 4, the statistical capacity distributions of an EV-Taxi were shown in two-dimensional space. In Figure 5, the statistical capacity distributions of an EV in Urban Dynamometer Driving Schedule (UDDS) were shown in one-dimensional space. From both of them we can see that most of these capacities converged into several

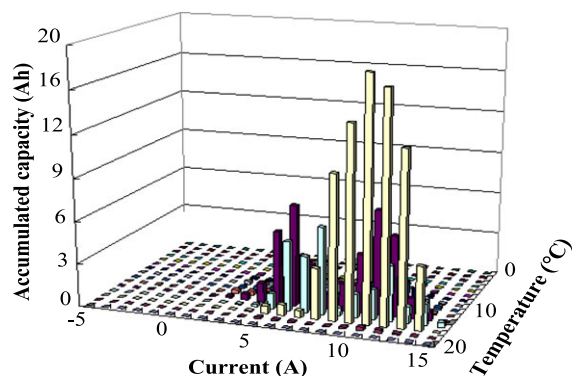


Figure 4. The capacity distributions in working conditions.

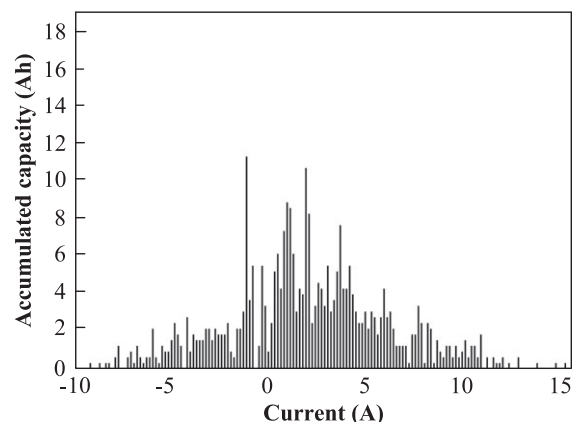


Figure 5. The capacity distributions in UDDS cycle.

special lattices. Thus, by collecting these discretized capacities, we can obtain the distribution information of them.

In fact, many algorithms can be used to calculate the accumulated capacities for lattices. The basic one is to book the same number of memory for lattices and update the accumulated capacities with the coming new records (I(t), T(t), SOC(t), SOH(t)) at each measurement point. When the granularities of these lattices are set to small values, the memory and calculation cost of it will be very large. But a small granularity will benefit the estimated results. To deal with this dilemma, several data-stream-mining based algorithm can be used for accumulating the discharged/charge capacities for lattices [31,32]. For example, Lossy counting and Sticky sampling are two methods that can be used for approximating the accumulated capacities with very small memory and computing requirements [33].

4.3. Estimating SOC or RC for batteries

For an EV, having initialized the initial SOC(t_0) in charging or open-circuit stage, we can estimate the SOC or RC

$$\begin{cases} (SOC(t_{k-Ln+1}) - SOC(t_{k-Ln+2})) \times C_N = \eta_{L1,k+1} \cdot Q_{L1,k-Ln+1} + \eta_{L2,k+1} \cdot Q_{L2,k-Ln+1} + \dots + \eta_{Ln,k+1} \cdot Q_{Ln,k-Ln+1} \\ (SOC(t_{k-Ln+2}) - SOC(t_{k-Ln+3})) \times C_N = \eta_{L1,k+1} \cdot Q_{L1,k-Ln+2} + \eta_{L2,k+1} \cdot Q_{L2,k-Ln+2} + \dots + \eta_{Ln,k+1} \cdot Q_{Ln,k-Ln+2} \\ \dots \\ (SOC(t_k) - SOC(t_{k+1})) \times C_N = \eta_{L1,k+1} \cdot Q_{L1,k} + \eta_{L2,k+1} \cdot Q_{L2,k} + \dots + \eta_{Ln,k+1} \cdot Q_{Ln,k} \end{cases} \quad (12)$$

of it with the proposed algorithm at any discharging time. The real-time capacities 'Q_{L1}, Q_{L2}, ..., Q_{Ln}' for lattices 'L1, L2, ..., Ln' are used to calculate the current SOC(t) with a formula below.

$$SOC(t) \approx SOC(t_0) - \frac{1}{C_N} [\eta_{L1} \cdot Q_{L1} + \eta_{L2} \cdot Q_{L2} + \dots + \eta_{Ln} \cdot Q_{Ln}]$$

where ' $\eta_{L1}, \eta_{L2}, \dots, \eta_{Ln}$ ' are the revised coulombic efficiencies. The residual capacity, Cr, of this battery can be obtained by,

$$Cr \approx (SOC(t_0) - SOC(t)) \times C_N$$

The rated capacity, C_N, can be obtained from the battery manufacturer. After a long-term running, it can also be measured by a standard discharging process in laboratory.

5. RE-CALIBRATING THE COULOMBIC EFFICIENCY, η

The vector of coulombic efficiency, $\eta = \{\eta_{L1}, \eta_{L2}, \dots, \eta_{Ln}\}$, keeps unchanged in the whole discharging stage. Every time a charging stage or an open circuit stage arrives, it will be updated with the historical capacity

distribution information and the new obtained capacity distribution information. Let Ln be the number of lattices, k be the number of the completed discharging cycles and SOC(t_{k+1}) be the current SOC obtained in the current charging/open-circuit stage. The updating process can be expressed like this,

- (1) Calculating the real-time SOC, SOC(t_{k+1}), at time t_{k+1} . (the calculation methods can be seen in section 3.1 or 3.2).
- (2) Reading in the nearest Ln times historical capacity-distribution-information in the discharging stages.

$$\begin{cases} Q_{L1,k-Ln+1}, Q_{L2,k-Ln+1}, \dots, Q_{Ln,k-Ln+1} & \text{(the } k-Ln+1 \text{ time),} \\ \dots \\ Q_{L1,k-1}, Q_{L2,k-1}, \dots, Q_{Ln,k-1} & \text{(the } k-1 \text{ time),} \\ Q_{L1,k}, Q_{L2,k}, \dots, Q_{Ln,k} & \text{(the } k \text{ time),} \end{cases} \quad (11)$$

- (3) Building the coulombic efficient updating matrix with the capacities and historical SOC values.

- (4) Calculating the coulombic efficiency vector with least square method and updating the old vector, $\eta_k = \{\eta_{L1,k}, \eta_{L2,k}, \dots, \eta_{Ln,k}\}$ with $\eta_{k+1} = \{\eta_{L1,k+1}, \eta_{L2,k+1}, \dots, \eta_{Ln,k+1}\}$.

6. VERIFICATION OF THE PROPOSED ESTIMATION METHOD

6.1. The test bench

The test bench is shown in Figure 6, which consists of a thermal chamber for environment control, a host computer, a BaTe battery test system NBT BTS5200C4 and BeltControl 2.0 interface for programming the NBT BTS5200C4. The maximum voltage, maximum charge/discharge current, current control accuracy and voltage control accuracy of NBT BTS5200C4 were 5.0 V, 200A, $\pm(0.1 \%FD + 0.1 \%RD)$ and $\pm(0.1 \%FD + 0.1 \%RD)$. In fact, the device can record the experiment data include temperature, current, voltage, accumulative amp-hours (Ah) and watt-hours (Wh). The host computer can collect the data through RS232/RS485 protocol.

6.2. The verification process

Figure 7 illustrates the process of the verification experiment for checking the accuracy of the LS based SOC estimation

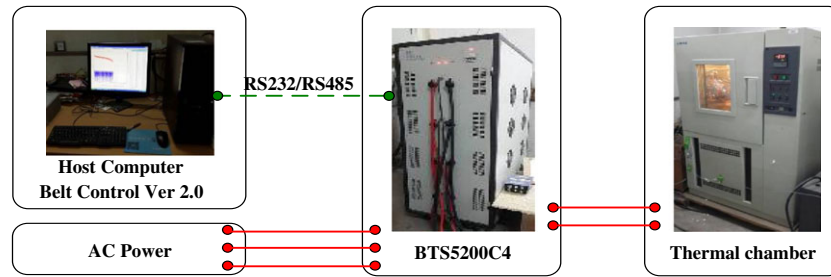


Figure 6. The battery test bench.

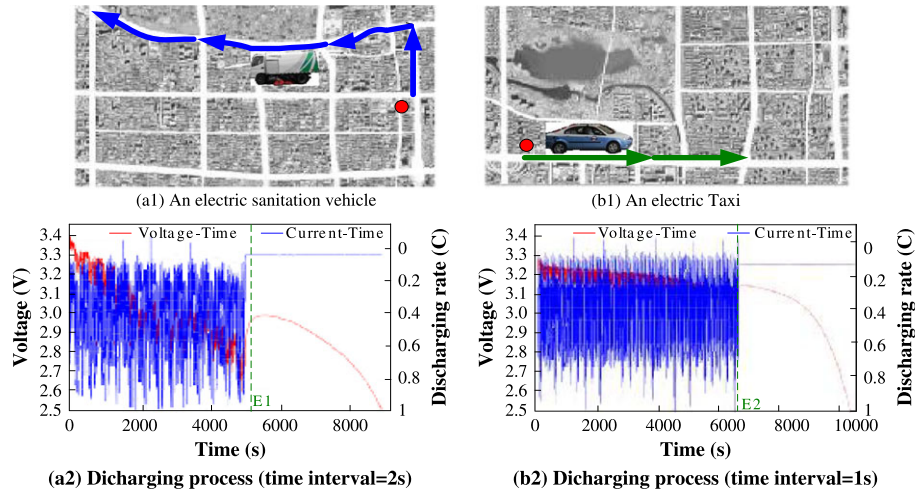


Figure 7. Two different discharging processes.

method. Two kinds of discharging cycles were used for testing the proposed algorithm. The first kind of driving cycles (consisting of 50 times running) was acquired in the city of Beijing in February and March of 2014. The electric Sanitation Vehicle used for generating these driving cycles is ZLJ5071TSL, the equipment number of which is 400. The second kind of driving cycles (consisting of 50 times running) was acquired in October and November of 2014, an electric Taxi ('B1Y048') was used for generating these driving cycles. The acquiring processes can be seen in Figure 7(a1) and (b1). Both of the two cycles made up of only city ways, the peak speeds of the electric sanitation vehicle and the electric Taxi are 35 km/h and 80 km/h.

Having obtained these driving cycles, the verification experiments were carried out on the test bench. The battery current is negative for charging, positive for discharging. Both of the experiments were carried out at 10 °C. The current, voltage and operating time were examined every 2 s in experiment

(a2), every 1 s in experiment (b2). Before the examined points (E1 and E2), the discharging process was carried out with the giving driving cycles. After them, the battery was discharged at 0.1C (2A) to the cut-off voltage (2.5 V). The discharge rate was discretized into 10 lattices, and 10 coulombic efficiency coefficients was initialized to 1 for the first driving cycle. After it, these coulombic efficiencies were updated every time a new driving cycle comes. The estimated equivalent discharged capacity at the examined point E1, $Q_{i,(0-E1)}$, can be calculated by,

$$Q_{i,(0-E1)} = \eta_{0-2A} \cdot Q_{0-2A,i} + \eta_{2-4A} \cdot Q_{2-4A,i} + \dots + \eta_{18-20A} \cdot Q_{18-20,i}$$

After 10 times of discharging cycles, we obtained the equations set below,

In both of the two experiments, the available capacity C_N was defined as the discharged capacity of the battery at the

$$\begin{cases} Q_{1,(0-E1)} = \eta_{0-2A,1} \cdot Q_{0-2A,1} + \eta_{2-4A,1} \cdot Q_{2-4A,1} + \dots + \eta_{18-20A,1} \cdot Q_{18-20A,1} \\ Q_{2,(0-E1)} = \eta_{0-2A,2} \cdot Q_{0-2A,2} + \eta_{2-4A,2} \cdot Q_{2-4A,2} + \dots + \eta_{18-20A,2} \cdot Q_{18-20A,2} \\ \dots \\ Q_{i,(0-E1)} = \eta_{0-2A,i} \cdot Q_{0-2A,i} + \eta_{2-4A,i} \cdot Q_{2-4A,i} + \dots + \eta_{18-20A,i} \cdot Q_{18-20A,i} \\ \dots \\ Q_{10,(0-E1)} = \eta_{0-2A,10} \cdot Q_{0-2A,10} + \eta_{2-4A,10} \cdot Q_{2-4A,10} + \dots + \eta_{18-20A,10} \cdot Q_{18-20A,10} \end{cases} \quad (13)$$

discharging current 2A. The operating temperature is 10 °C. Thus, for each of the discharge cycle i , the true equivalent discharged capacity of it at the examined point E1, $Q_{i, (0-E1)}$, can be expressed by $Q_{i, (0-E1)} = C_N - Q_{i, (E1-END)}$. $Q_{i, (E1-END)}$ is the discharge capacity of the battery at 2A (from time E1 to the end). In this way, equation set (13) can be changed into (14). ϵ_i is the error between the real RC and the estimated RC.

$$\begin{cases} C_N - Q_{1, (E1-END)} = \eta_{0-2A,1} \cdot Q_{0-2A,1} + \eta_{2-4A,1} \cdot Q_{2-4A,1} + \dots + \eta_{18-20A,1} \cdot Q_{18-20A,1} + \epsilon_1 \\ C_N - Q_{2, (E1-END)} = \eta_{0-2A,2} \cdot Q_{0-2A,2} + \eta_{2-4A,2} \cdot Q_{2-4A,2} + \dots + \eta_{18-20A,2} \cdot Q_{18-20A,2} + \epsilon_2 \\ \dots \\ C_N - Q_{i, (E1-END)} = \eta_{0-2A,i} \cdot Q_{0-2A,i} + \eta_{2-4A,i} \cdot Q_{2-4A,i} + \dots + \eta_{18-20A,i} \cdot Q_{18-20A,i} + \epsilon_i \\ \dots \\ C_N - Q_{10, (E1-END)} = \eta_{0-2A,10} \cdot Q_{0-2A,10} + \eta_{2-4A,10} \cdot Q_{2-4A,10} + \dots + \eta_{18-20A,10} \cdot Q_{18-20A,10} + \epsilon_{10} \end{cases} \quad (14)$$

Thus, if we initialize the coulombic efficiency, $\eta = \{\eta_{0-2A}, \dots, \eta_{18-20A}\}$, with 1 in the first 10 equations, and accumulate the capacities for lattices in each discharge cycle. After ten times running, the accurate coulombic efficiencies will be obtained with formula (13) and (14), gradually.

In Figure 8, two kinds of coulomb counting methods were shown. The solid line shows the errors (ϵ_i) between the real RC and the estimated RC, which is obtained with the proposed algorithm (Algorithm-2). The dash line shows the estimated error obtained with the basic coulomb counting method (Algorithm-1). From it we can find that, in the former ten driving cycles, both of the errors obtained with the two algorithms keep similar. The values of them in (a) are nearly 4%, in (b) are nearly 6%. However, after 10 times of implementations, the obtained results with the two algorithms were so different. For Algorithm-1, because no correction was carried out on the coulombic efficiencies, the estimation errors kept almost unchanged. For Algorithm-2, by introducing the self-adapting coulombic efficiencies, $\eta = \{\eta_{0-2A}, \eta_{2-4A}, \dots, \eta_{18-20A}\}$, the estimation errors reduced to nearly 2.5% and 3%.

6.3. The influences of noise

As a characteristic of all electronic circuits, noise is a random fluctuation in an electrical signal and can be produced by several different effects, such as device type, manufacturing quality and semiconductor defects. To further examine the influences of the sensor noise, two kinds of noise were

overlaid on the original current signals. In the first kind of noise, the mathematical expectation of which is zero. It was utilized to show the random error of the sensor and its amplitude was set to $[-0.1A-0.1A]$. In the second kind of noise, the mathematical expectation of which was set to a nonzero value. It was used to show the inherent error of the sensor, and its amplitude was set to $[-0.1A-0.2A]$.

After 50 discharge/charge cycles, the accumulated errors of these discharging cycles were shown in Figure 9, from which we can see that, although the obtained current information were overlaid with the same noise signal, δ , the relative errors of the traditional coulomb counting method (algorithm-1) and the proposed coulomb counting method (algorithm-2) were so different. When noise $[-0.1A-0.1A]$ was overlaid on the original current signals, the trends of the relative errors obtained with the two methods keep stable (comparing with Figure 8). However, when noise $[-0.1A-0.2A]$ was overlaid on the original current signals, the relative errors obtained with Algorithm-1 increased. But the trend of the relative errors obtained with Algorithm-2 first increased, and then, decreased to its original level. What is the reason?

The answer lies in the equation set (14). When noise $[-0.1A-0.2A]$ was overlaid on the original current signals, all of the accumulated capacities for lattices L_n , $Q_{L_n,i}$ were decreased. In the former 10 RC calculation, the coulombic efficiency, $\eta_{L_n,i}$, for each lattice cannot be revised. So, the obtained errors increased. However, after 10 times running (10 equations), the coulombic efficiency, $\eta_{L_n,i}$, began to be revised dynamically. Although the coulombic efficiencies, $\eta_{L_n,i}$, were changed into morbid values as the polluted capacities, $Q_{L_n,i}$, were introduced, the ultimate estimation error was very small because of the interaction effects. The specific changing process can be seen in Figure 10, where the values of two coulombic efficiency, $\eta_{[4A-6A]}$ and $\eta_{[8A-10A]}$, of the verification experiment-2 (Taxi) were shown in (a1) and (b1).

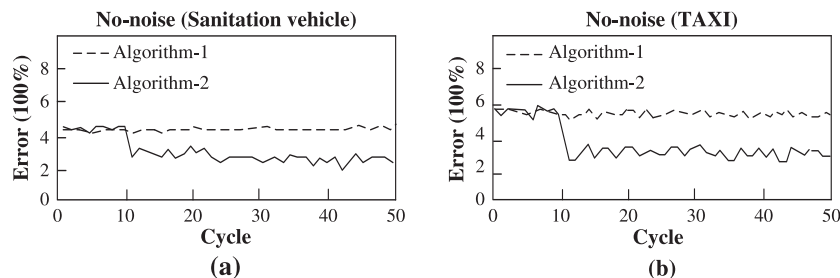


Figure 8. Estimation errors of various coulomb counting methods.

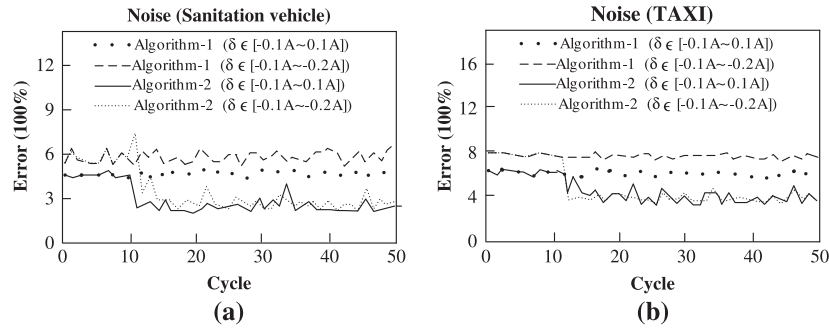


Figure 9. Estimation errors of various coulomb counting methods in noise conditions.

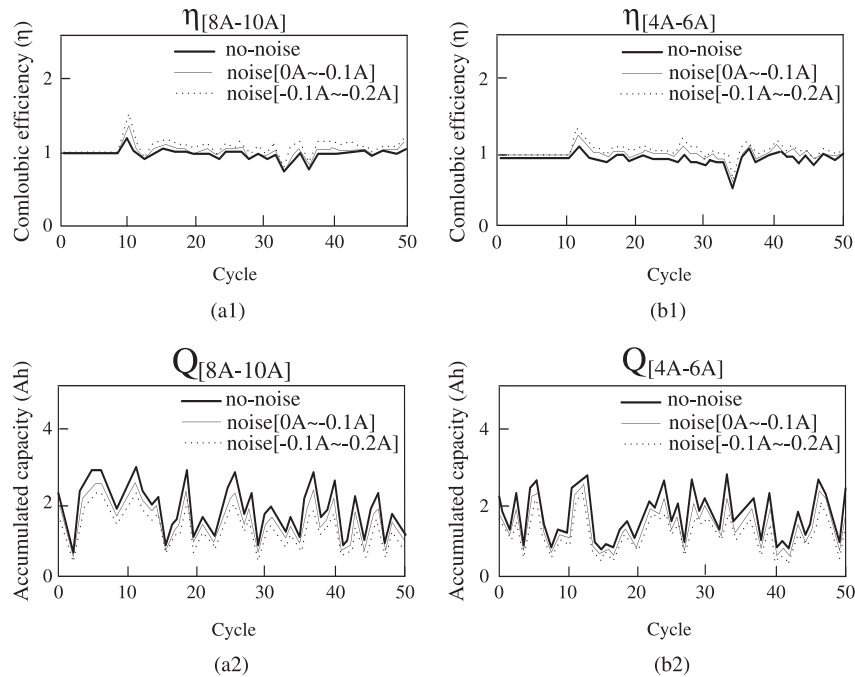


Figure 10. The relative errors in different noisy environments.

And the corresponding accumulated capacities, $Q_{[4A-6A]}$ and $Q_{[8A-10A]}$ were shown in (a2) and (b2).

It can be found that, with the intervention of the noise $[-0.1A - -0.2A]$, the accumulated capacities, $Q_{[4A-6A]}$ and $Q_{[8A-10A]}$, decreased in the total 50 driving cycles. However, the corresponding coulombic efficiencies, $\eta_{[4A-6A]}$ and $\eta_{[8A-10A]}$, kept unchanged in the former 10 time running and increased in the later 40 time running. Because no revision was carried out in the former 10 driving cycles (the values of $\eta_{[4A-6A]}$ and $\eta_{[8A-10A]}$ kept unchanged), the relative errors obtained in the former 10 driving cycles were larger than that in the latter 40 driving cycles.

7. CONCLUSION

In this paper, we have demonstrated advanced strategy for re-calibrating the coulombic efficiency. The leading idea

was to build a coulombic efficiency matrix with statistical information and to compensate the cumulative errors with the morbid coulombic efficiencies. The key method to calculate the matrix was least square, and the proposed SOC estimation method (coulomb counting method) was largely based on it.

The results indicate that the proposed algorithm has the capabilities of correcting the cumulative errors coming from measurement drifts and estimating the RC with more accurate coulombic efficiencies. It largely reduces the cost of the current sensor and complexity of the circuit.

We showed the root cause of the errors coming from a traditional coulomb counting method (Ampere-Hour integral method) and given the principles/usages of the proposed algorithm. The initial SOC is calculated in open circuit stage or charging stage. The estimation of SOC/RC and the modification of coulombic efficiencies are carried out in the discharging stage.

We found that, for an EV, the inherent errors coming from sensors or other measuring equipment cannot be revised by traditional coulomb counting method, but can be revised by the proposed method. Additionally, in a short-running process, the coulombic efficiency of a battery in EV was largely decided by discharge/charge current and temperature, slightly decided by available capacity and other factors.

In conclusion, estimating SOC/RC for an EV with the method described in this paper will help improving the accuracy of SOC estimation.

ACKNOWLEDGEMENTS

We are grateful to the anonymous referees for their invaluable suggestions to improve the paper. This work was supported by the National Natural Science Foundation of China (51275053), And it is sponsored by the State Key Laboratory of Automotive Safety and Energy under Project No. KF16032.

REFERENCES

- Kang J, Rizzoni G. Study of relationship between temperature and thermal energy, operating conditions as well as environmental factors in large-scale lithium-ion batteries. *International Journal of Energy Research* 2014; **38**:1994–2002.
- Akhtar N, Akhtar W. Prospects, challenges, and latest developments in lithium-air batteries. *International Journal of Energy Research* 2015; **39**:303–316.
- Lu L, Han X, Li J. A review on the key issues for lithium-ion battery management in electric vehicles. *Journal of Power Sources* 2013; **226**:272–288.
- Lindgren J, Niemi R, Lund PD. Effectiveness of smart charging of electric vehicles under power limitations. *International Journal of Energy Research* 2014; **38**:404–414.
- Chabot V, Farhad S, Chen Z. Effect of electrode physical and chemical properties on lithium-ion battery performance. *International Journal of Energy Research* 2013; **37**:1723–1736.
- Karimi G, Li X. Thermal management of lithium-ion batteries for electric vehicles. *International Journal of Energy Research* 2013; **37**:13–24.
- Jin B, Sun G, Liang J. Physicochemical properties of lithium iron phosphate-carbon as lithium polymer battery cathodes. *International Journal of Energy Research* 2013; **37**:500–509.
- Ranjbar AH, Banaei A, Khoobroo A, Fahimi B. Online estimation of state of charge in Li-ion batteries using impulse response concept. *IEEE Transactions On Smart Grid* 2012; **3**:360–367.
- Arora P, White RE, Doyle M. Capacity fade mechanisms and side reactions in lithium-ion batteries. *Journal of the Electrochemical Society* 1998; **145**:3647–3667.
- Zhang X. Thermal analysis of a cylindrical lithium-ion battery. *Electrochimica Acta* 2011; **56**:1246–1255.
- Sakti A, Michalek J, Jeremy J. A validation study of lithium-ion cell constant c-rate discharge simulation with Battery Design Studio (R). *International Journal of Energy Research* 2013; **37**:1562–1568.
- Zheng Y, Lu L, Han X. LiFePO₄ battery pack capacity estimation for electric vehicles based on charging cell voltage curve transformation. *Journal of Power Sources* 2013; **226**:33–41.
- Xing Y, He W, Pecht M, Tsui KL. State of charge estimation of lithium-ion batteries using the open-circuit voltage at various ambient temperatures. *Applied Energy* 2014; **113**:106–115.
- He H, Qin H, Sun X, Shui Y. Comparison study on the battery SoC estimation with EKF and UKF algorithms. *Energies* 2013; **6**:5088–5100.
- Li Y, Liao C, Wang L. Subspace-based modeling and parameter identification of lithium-ion batteries. *International Journal of Energy Research* 2014; **38**:1024–1038.
- Cho S, Jeong H, Han C, Jin S, Lim JH, Oh J. State-of-charge estimation for lithium-ion batteries under various operating conditions using an equivalent circuit model. *Computers & Chemical Engineering* 2012; **41**:1–9.
- Li IH, Wang WY, Su SF, Lee YS. A merged fuzzy neural network and its applications in battery state-of-charge estimation. *IEEE Transactions On Energy Conversion* 2007; **22**:697–708.
- Affanni A, Bellini A. Battery choice and management for new generation electric vehicles. *IEEE Transactions on Industrial Electronics* 2005; **52**(5):1343–9.
- Lin C, Chen QS, Wang JP, et al. Improved Ah counting method for state of charge estimation of electric vehicle batteries. *Journal of Tsinghua University (Sci&Tech)* 2006; **46**:247–251.
- Pei F, Zhao K, Luo Y. Battery variable current-discharge resistance characteristics and state-of-charge estimation of electric vehicle. *Proc IEEE World Congress Intell Control Automat* 2006; **2**:8314–8322.
- Pop V, Bergveld HJ, et al. State-of-charge indication in portable applications. *Proc Int Symp on Ind Electron* 2005; **3**:1007–1019.
- Wang J, Cao B, Chen Q, Wang F. Combined state of charge estimator for electric vehicle battery pack. *Control Engineering Practice* 2007; **15**:1569–1576.
- Ng KS, Moo C-S, Chen Y-P, Hsieh Y-C. Enhanced coulomb counting method for estimating state-of-

- charge and state-of-health of lithium-ion batteries. *Applied Energy* 2009; **86**:1506–1511.
24. Hansen T, Wang CJ. Support vector based battery state of charge estimator. *Journal of Power Sources* 2005; **141**:351–358.
 25. Wang JP, Chen QS, Cao BG. Support vector machine based battery model for electric vehicles. *Energy Conversion and Management* 2006; **47**(7):858–864.
 26. Ye Y, Shi Y, Cai N, Lee J, He X. Electro-thermal modeling and experimental validation for lithium ion battery. *Journal of Power Sources* 2012; **199**:227–238.
 27. Zhang X, Kong X, Li G, Li J. Thermodynamic assessment of active cooling/heating methods for lithium-ion batteries of electric vehicles in extreme conditions. *Energy* 2014; **64**:1092–1101.
 28. Ye Y, Shi Y, Tay AAO. Electro-thermal cycle life model for lithium iron phosphate battery. *Journal of Power Sources* 2012; **217**:509–518.
 29. Saw L, Ye Y, Tay A. Electrochemical–thermal analysis of 18,650 Lithium Iron Phosphate cell. *Energy Conversion and Management* 2013; **75**:162–174.
 30. Mohammad Rezvanizani S, Liu Z, Chen Y, Lee J. Review and recent advances in battery health monitoring and prognostics technologies for electric vehicle (EV) safety and mobility. *Journal of Power Sources* 2014; **256**:110–124.
 31. Nasraoui O, Rojas C, Cardona C. A framework for mining evolving trends in Web data streams using dynamic learning and retrospective validation. *Journal of Computer Networks—Special Issue on Web Dynamics* 2006; **50**(10):1425–1652.
 32. Zhao L, Wang L, Xu Q. Data stream classification with artificial endocrine system [J]. *Applied Intelligence* 2012; **37**(3):390–404.
 33. R Motwani, GS Manku. Approximate frequency counts over data streams. VLDB '02 Proceedings of the 28th international conference on Very Large Data Bases: 2002; 346–357.